STATISTICAL PROPERTIES OF THE RADIATION FROM SASE FEL OPERATING IN A POST-SATURATION REGIME WITH AND WITHOUT UNDULATOR TAPERING

E.A. Schneidmiller, M.V. Yurkov, DESY, Hamburg, Germany

Abstract

We describe statistical and coherence properties of the radiation from x-ray free electron lasers (XFEL) operating in the post-saturation regime. We consider practical case of the SASE3 FEL at European XFEL. We perform comparison of the main characteristics of X-ray FEL operating in the post-saturation regime with and without undulator tapering: efficiency, coherence time and degree of transverse coherence.

INTRODUCTION

Radiation from Self Amplified Spontaneous Emission Free Electron Laser (SASE FEL) [1, 2] has limited spatial and temporal coherence. This happens due to start-up of the amplification process from the shot noise in the electron beam. The fluctuations of the electron beam density are uncorrelated in time and space, and many radiation modes are excited at the initial stage of amplification. As a rule, ground spatial TEM_{00} mode with highest gain dominates, and the degree of transverse coherence grows in the exponential amplification stage. Radiation wave slips forward with respect to the electron beam by one wavelength per one undulator period. This relative slippage on the scale of the field gain length gives an estimate for coherence length. Both, degree of transverse coherence and coherence time reach maximum value in the end of the exponential regime of amplification, and then degrade visibly in the nonlinear regime. Maximum degree of transverse coherence of about 0.95 is reached for the values of diffraction parameter about 1. For large values of the diffraction parameter the degree of transverse coherence falls down due to poor mode selection, i.e. mode degeneration takes place. For small values of the diffraction parameter the degree of transverse coherence falls down due to more poor longitudinal coherence [3–6].

Radiation from SASE FEL with planar undulator contains visible contribution of odd harmonics. Parameter range where intensity of higher harmonics is defined mainly by nonlinear beam bunching in the fundamental harmonic has been intensively studied in refs. [7–16]. Comprehensive studies of the nonlinear harmonic generation have been performed in [16] in the framework of the one-dimensional model. General features of harmonic radiation have been determined. It was found that coherence time at saturation falls inversely proportional to harmonic number, and relative spectrum bandwidth remains constant with harmonic number. Comprehensive study of the coherence properties of the odd harmonics in the framework of 3D model have been performed in [17]. We considered parameter range when intensity of higher harmonics is mainly defined by nonlinear harmonics generation mechanism. The case optimized XFEL has been considered. Using similarity techniques we present universal dependencies for the main characteristics of the SASE FEL covering all practical range of optimized X-ray FELs.

Application of the undulator tapering [18] allows to increase conversion efficiency to rather high values [19–27]. New wave of interest to the undulator tapering came with x-ray free electron lasers [28–32] (see [33–36] and references therein). It is used now not only as demonstration tool [37], but as a routine tool at operating x-ray FEL facilities LCLS and SACLA.

There are several reasons why we performed the present study. The first reason is that SASE3 FEL at the European XFEL operating at long wavelengths can not be tuned as optimized FEL [4] due to limitation on minimum value of the focusing beta function, and dedicated study is required for description of coherence properties. Another reason is that in the parameter range of SASE3 FEL linear mechanism of harmonic generation is essential which results in much higher power of higher odd harmonic with respect to the case of nonlinear harmonic generation [33, 38]. Finally, we compare coherence properties for both, fundamental and the third harmonic for the case of untapered undulator and undulator with optimized tapering. We show that the brilliance of the fundamental harmonic of the radiation from SASE FEL with optimized tapering can be increased by a factor of 3 with respect to untapered case.

GENERAL DEFINITIONS AND SIMULATION PROCEDURE

The first-order transverse correlation function is defined as

$$\gamma_1(\vec{r}_\perp,\vec{r}\,'_\perp,z,t)=\frac{\langle\tilde{E}(\vec{r}_\perp,z,t)\tilde{E}^*(\vec{r}\,'_\perp,z,t)\rangle}{\left[\langle|\tilde{E}(\vec{r}_\perp,z,t)|^2\rangle\langle|\tilde{E}(\vec{r}\,'_\perp,z,t)|^2\rangle\right]^{1/2}},$$

where $\tilde{E}$ is the slowly varying amplitude of the amplified wave. For a stationary random process γ_1 does not depend on time, and the degree of transverse is:

$$\zeta=\frac{\int|\gamma_1(\vec{r}_\perp,\vec{r}\,'_\perp)|^2 I(\vec{r}_\perp)I(\vec{r}\,'_\perp)\,\mathrm{d}\vec{r}_\perp\,\mathrm{d}\vec{r}\,'_\perp}{[\int I(\vec{r}_\perp)\,\mathrm{d}\vec{r}_\perp]^2},$$

where $I(\vec{r}_\perp)=\langle|\tilde{E}(\vec{r}_\perp)|^2\rangle$. The first order time correlation function, $g_1(t,t')$, is calculated in accordance with the definition:

$$g_1(\vec{r},t-t') = \frac{\langle \tilde{E}(\vec{r},t)\tilde{E}^*(\vec{r},t')\rangle}{\left[\langle|\ \tilde{E}(\vec{r},t)\ |^2\rangle\langle|\ \tilde{E}(\vec{r},t')\ |^2\rangle\right]^{1/2}} ,$$

For a stationary random process time correlation functions are functions of the only argument, $\tau = t - t\prime$. The coherence time is defined as $\tau_c = \int_{-\infty}^{\infty} |g_1(\tau)|^2 \, \mathrm{d}\,\tau$. Peak brilliance is defined as a transversely coherent spectral flux:

$$B = \frac{\omega \, \mathrm{d}\, \dot{N}_{ph}}{\mathrm{d}\,\omega} \frac{\zeta}{(\lambda/2)^2} .$$

If one traces evolution of the brilliance of the radiation along the undulator length there is always the point, which we define as the saturation point, where the brilliance reaches maximum value [4].

Simulations have been performed with three-dimensional, time-dependent FEL simulation code [4, 17, 39] tracing actual number of electrons. In our simulation procedure particles correspond to real electrons randomly distributed in full 6D phase space. This allows us to avoid any artificial effects arising from standard procedures of macroparticle loading as we described earlier [4]. Simulations of the FEL process have been performed for the case of a long bunch with uniform axial profile of the beam current. Such a model provides rather accurate predictions for the coherence properties of the XFEL, since typical radiation pulse from the XFEL is much longer than the coherence time. Output of the simulation code are arrays containing complex values of the radiation field amplitudes. Then we apply statistical analysis, and calculate physical values as it has been defined in this section.

RESULTS

We perform comparative analysis of tapered and untapered case for parameters of the SASE3 undulator of the European XFEL. Undulator period is 6.8 cm, electron energy is 14 GeV, radiation wavelength is 1.55 nm. Undulator consists of 21 modules, each is 5 meters long with 1.1 m long intersections between modules. Parameters of the electron beam correspond to 0.25 nC case of the baseline parameters of the electron beam: emittance 0.6 mm-mrad, rms energy spread 2.5 MeV, peak beam current 5 kA [33]. Average focusing beta function is equal to 15 m. The value of the diffraction parameter is B = 1.1 which is close to optimum conditions for reaching maximum value of the degree of transverse coherence [4]. Two cases were simulated: untapered undulator, and undulator optimized for maximum FEL efficiency [40].

Plots in Fig. 1 show evolution along the undulator of the radiation power, degree of transverse coherence, coherence time, and brilliance for the fundamental harmonic. Power, coherence time, and brilliance are normalized to the values

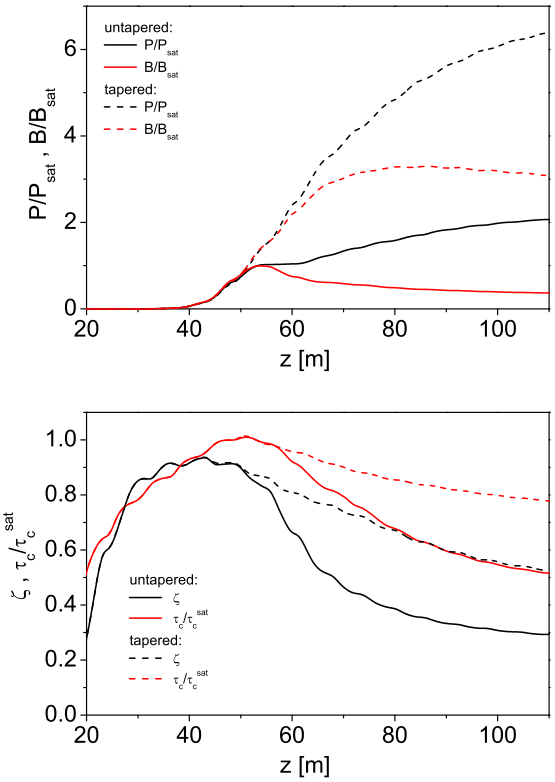

Figure 1: Fundamental harmonic: evolution of the radiation power and brilliance (top plot) and of coherence time and degree of transverse coherence (bottom plot) along the undulator for untapered (solid curves) and optimized tapered case (dashed curves).

of the fundamental harmonic in the saturation point. Saturation length for the fundamental harmonic is equal to 53 m. Absolute values in the saturation point are: radiation power is 108 GW and 6.6 GW; coherence time is 1.2 fs and 0.5 fs; degree of transverse coherence is 0.86 and 0.72 for the fundamental and the 3rd harmonic, respectively. Brilliance of the fundamental harmonic in the saturation point is equal to 3.8×10^{22} photons/sec/mm^2/rad^2/0.1% bandwidth. Now we compare behavior of the radiation properties for the tapered and untapered case. Growth of the radiation power is higher for the tapered case. We also obtain less intensive degradation of the coherence properties of the radiation. However, brilliance of the radiation for tapered saturates at the undulator length of 80 m, and then drops down gradually. Benefit of the tapered case against untapered case in terms of the radiation brilliance is factor of 3. It is mainly reached by the increase of the radiation power by a factor of 5. Coherence properties of the radiation in the point of maximum brilliance are worse than those of the untapered SASE FEL in the saturation point: 0.86 to 0.68 for the degree of transverse coherence, and 1 to 0.86 in terms of coherence time. Figure 2 presents normalized spectral power of the fundamental harmonic for untapered (black) and tapered (red) case. Output points correspond to the maximum

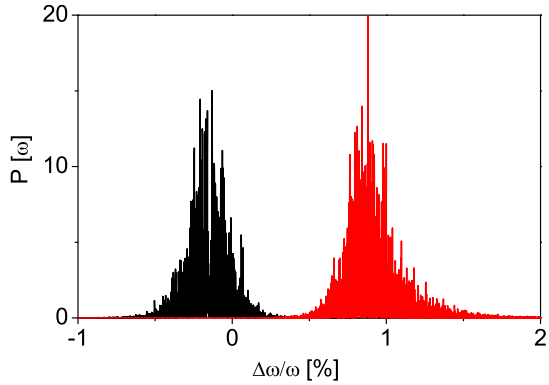

Figure 2: Normalized spectral power of the fundamental harmonic for untapered (black) and tapered (red) case. Output points correspond to the maximum brilliance: $z = 53$ m and $z = 80$ m for untapered and tapered case, respectively. Spectrum of untapered case is shifted by 1% to the right-hand side.

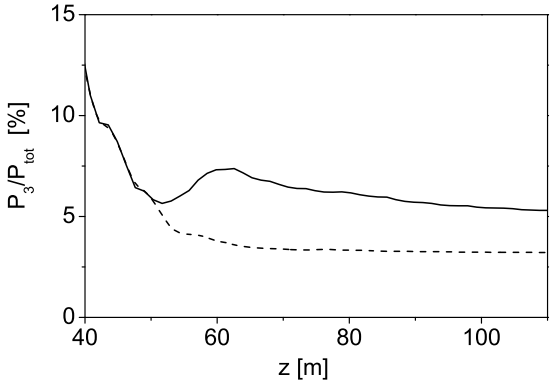

Figure 3: Contribution of the 3rd harmonic radiation power to the total radiation power for untapered (solid curves) and optimized tapered case (dashed curves).

brilliance: $z = 53$ m and $z = 80$ m for untapered and tapered case, respectively. It is seen that spectrum of the untapered case is more narrow and does not contain spanning tails.

We already mentioned that parameters of SASE3 FEL are such that we expect significant increase of the radiation power in the higher odd harmonics due to mechanism of linear harmonic generation. This happens due to small value of the diffraction parameter and high quality of the electron beam (small emittance and energy spread) [38]. Results of numerical simulations presented in Fig. 3 shows that for untapered case contribution of the 3rd harmonic to the total power is about 6% in the saturation point. Note that mechanism of nonlinear harmonic generation results in the value of 2% only. High value of the 3rd harmonic radiation power should be the subject of concern for the planned user experiments. It can constitute harmful background, or can be used in pump-probe experiments. Mechanisms to control 3rd harmonic contribution are now the subject of dedicated studies [41].

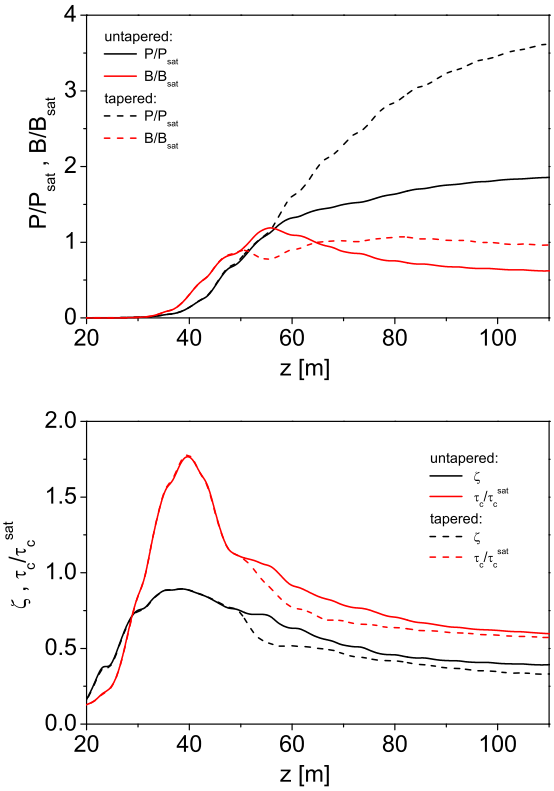

Figure 4: 3rd harmonic: evolution of the radiation power and brilliance (top plot) and of coherence time and degree of transverse coherence (bottom plot) along the undulator for untapered (solid curves) and optimized tapered case (dashed curves).

Plots in Fig. 4 show evolution along the undulator of the radiation power, degree of transverse coherence, coherence time, and brilliance for the 3rd harmonic. Power, coherence time, and brilliance are normalized to the values of the 3rd harmonic in the saturation point of the fundamental harmonic. Absolute numbers were introduced above. There is interesting observation that brilliance of the radiation of the 3rd harmonic does not differ significantly for untapered and tapered cases. In the case of optimized tapered undulator relative contribution of the 3rd harmonic to the total power is visibly less while absolute power is higher than for untapered case. Coherence properties of the 3rd harmonic for untapered case are a bit better than those of the tapered case.

To make our paper complete, we conclude with presenting in Fig. 5 of the evolution along the undulator of the FWHM spot size and FWHM angular divergence of the radiation in the far zone. Cone of the fundamental harmonic radiation in the far zone is visibly wider for the tapered case. Also, phase front of the radiation is quite different for tapered and untapered case. This is a hint for careful design of the optical transport system capable effectively handle both, untapered and tapered options.

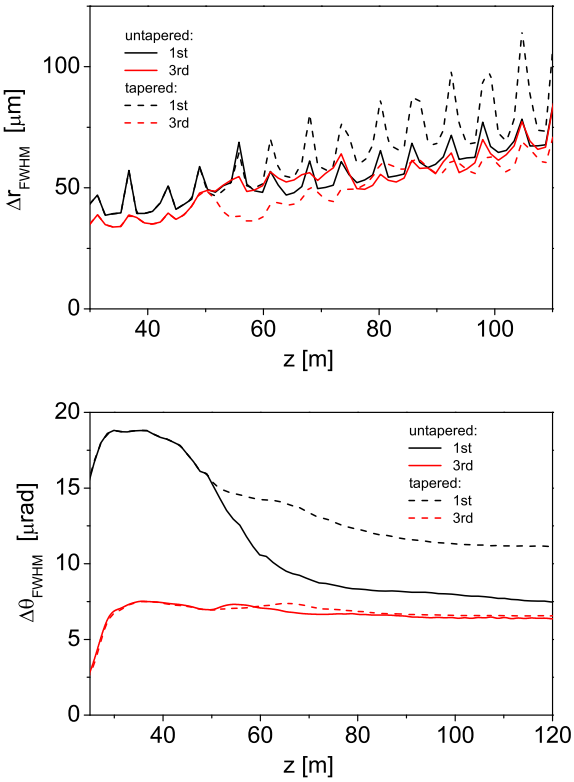

Figure 5: Evolution along the undulator of the FWHM spot size (top plot) and FWHM angular divergence of the radiation in the far zone (bottom plot) for untapered (solid curves) and optimized tapered case (dashed curves). Black and red colors correspond to the fundamental and the 3rd harmonic, respectively.

SUMMARY

Application of undulator tapering has evident benefit for SASE3 FEL operating in the wavelength range around 1.6 nm. It is about factor of 6 in the pulse radiation energy with respect to the saturation regime, and factor of 3 with respect to the radiation power at full length. General feature of tapered regime is that both, spatial and temporal coherence degrade in the nonlinear regime, but a bit slowly than for untapered case. Peak brilliance is reached in the middle of tapered section, and exceeds by a factor of 3 the value of the peak brilliance in the saturation regime. Degree of transverse coherence in the saturation for untapered case is 0.86. Degree of transverse coherence for maximum brilliance of tapered case is 0.66. Coherence time falls by 15%. At the exit of the undulator degree of transverse coherence for tapered case is 0.6, and coherence time falls by 20%. 3rd harmonic in the nonlinear regime for both, untapered and tapered cases, exhibit nearly constant brilliance and nearly constant contribution to the total power. Coherence time of the 3rd harmonic for the tapered case approximately scales inversely proportional to harmonic number, as in untapered case.

REFERENCES

[1] Ya.S. Derbenev, A.M. Kondratenko, and E.L. Saldin, Nucl. Instrum. and Methods 193 (1982) 415.

[2] J.B. Murphy and C. Pellegrini, Nucl. Instrum. and Methods A237 (1985) 159.

[3] E.L. Saldin, E.A. Schneidmiller, and M.V. Yurkov, Opt. Commun. **186** (2000) 185.

[4] E.L. Saldin, E.A. Schneidmiller, and M.V. Yurkov, Opt. Commun. 281 (2008) 1179.

[5] E.L. Saldin, E.A. Schneidmiller, and M.V. Yurkov, Opt. Commun. 281 (2008) 4727.

[6] E.L. Saldin, E.A. Schneidmiller, and M.V. Yurkov, New J. Phys. 12 (2010) 035010, doi: 10.1088/1367-2630/12/3/035010.

[7] M. Schmitt and C. Elliot, Phys. Rev. A, 34 (1986) 6.

[8] R. Bonifacio, L. De Salvo, and P. Pierini, Nucl. Instr. Meth. A 293 (1990) 627.

[9] W.M. Fawley, Proc. IEEE Part. Acc. Conf., 1995, p. 219.

[10] H. Freund, S. Biedron and S. Milton, Nucl. Instr. Meth. A 445 (2000) 53.

[11] H. Freund, S. Biedron and S. Milton, IEEE J. Quant. Electr. 36 (2000) 275.

[12] S. Biedron et al., Nucl. Instr. Meth. A 483 (2002) 94.

[13] S. Biedron et al., Phys. Rev. ST 5 (2002) 030701.

[14] Z. Huang and K. Kim, Phys. Rev. E, 62 (2000) 7295.

[15] Z. Huang and K. Kim, Nucl. Instr. Meth. A 475 (2001) 112.

[16] E.L. Saldin, E.A. Schneidmiller and M.V. Yurkov, Phys. Rev. ST-AB 9 (2006) 030702

[17] E.A. Schneidmiller and M.V. Yurkov, Proc. 2012 FEL Conference, Nara, Japan, 2012, p. 65.

[18] N.M. Kroll, P.L. Morton, and M.N. Rosenbluth, IEEE J. Quantum Electron. 17, 1436 (1981).

[19] T.J. Orzechowski et al., Phys. Rev. Lett. 57, 2172 (1986).

[20] R.A. Jong, E.T. Scharlemann, W.M. Fawley Nucl. Instrum. Methods Phys. Res. A272, 99 (1988).

[21] W.M. Fawley, Nucl. Instrum. Methods Phys. Res. A375, 550 (1996).

[22] W.M. Fawley et al., Nucl. Instrum. Methods Phys. Res. A483, 537 (2002).

[23] E.L. Saldin, E.A. Schneidmiller and M.V. Yurkov, Opt. Commun. 95, 141 (1993).

[24] Review by E.T. Scharlemann in Laser Handbook, Volume 6, Free electron lasers, eds. W.B. Colson, C. Peilegrini and A. Renieri (North Holland, Amsterdam, 1991).

[25] E.L. Saldin, E.A. Schneidmiller and M.V. Yurkov, Physics Reports 260, 187 (1995).

[26] E.L. Saldin, E.A. Schneidmiller, M.V. Yurkov, "The Physics of Free Electron Lasers" (Springer-Verlag, Berlin, 1999).

[27] E.A. Schneidmiller, V.F. Vogel, H. Weise and M.V. Yurkov, Journal of Micro/Nanolithogrphy, MEMS, and MOEMS 11(2), 021122 (2012).

[28] P. Emma et al., Nature Photonics **4** (2010) 641.

[29] T. Ishikawa et al., Nature Photonics 6 (2012) 540.

[30] M. Altarelli et al. (Eds.), XFEL: The European X-Ray Free-Electron Laser. Technical Design Report, Preprint DESY 2006-097, DESY, Hamburg, 2006 (see also http://xfel.desy.de).

[31] R. Ganter (Ed.), Swiss FEL Conceptual Design Report, PSI Bericht Nr. 10-04, April 2012.

[32] H.S. Kang, K.W. Kim, I.S. Ko, Current Status of PAL-XFEL Project. Proc. IPAC 2014 Conf., paper THPRO019 (2014).

[33] E.A. Schneidmiller and M.V. Yurkov, Preprint DESY 11-152, Hamburg, 2011.

[34] Y. Jiao et al. Phys. Rev. ST Accel. Beams 15, 050704 (2012).

[35] G. Geloni, V. Kocharyan, and E. Saldin, DESY Report 11-049, 2011.

[36] I. Agapov et al., Proc. 2014 FEL Conference, Basel, Switzerland, 2014, MOP056.

[37] Y Hidaka et al., Proceedings of 2011 Particle Accelerator Conference, New York, NY, USA, THP148 (2011).

[38] E.A. Schneidmiller and M.V. Yurkov, Phys. Rev. ST-AB **15** (2012) 080702.

[39] E.L. Saldin, E.A. Schneidmiller, and M.V. Yurkov, Nucl. Instrum. and Methods **A 429** (1999) 233.

[40] E.A. Schneidmiller and M.V. Yurkov, Proc. 2014 FEL Conference, Basel, Switzerland, 2014, MOP065.

[41] E.A. Schneidmiller and M.V. Yurkov, Proc. 2014 FEL Conference, Basel, Switzerland, 2014, MOP068.